Fuel 222 (2018) 810–820

Contents lists available at ScienceDirect

Fuel

journal homepage: www.elsevier.com/locate/fuel

Full Length Article

Modeling of macroscopic mineral diesel and biodiesel spray characteristics

Breda Kegl*, Luka Lešnik

University of Maribor, Faculty of Mechanical Engineering, Smetanova 17, SI-2000 Maribor, Slovenia

ARTICLE INFO

Keywords:
Modified model
Biodiesel
Spray length
Spray angle
Cavitation

ABSTRACT

This paper investigates the injection of fuel into a constant volume spray chamber at high pressures by utilizing macroscopic fuel spray characteristics of mineral diesel and rapeseed oil biodiesel. In the case of lower spray chamber pressure the shapes of fuel sprays tend to be more inclined and indicate higher cavitation inside the nozzle hole. On this basis and from experimentally obtained spray tip penetration and spray angle, a modified mathematical model for spray tip penetration and spray angle is developed. This new model includes two-zone theory and the obtained results agree very well with experiments through the whole interval of spray development.

1. Introduction

Modern diesel engines have to fulfill requirements regarding engine performance, fuel consumption and have to meet current and future ever-stronger emissions regulations. Harmful emissions, especially particulate matters and NO_x emissions, are highly dependent on the combustion process. The combustion process is significantly influenced by fuel injection process and by fuel/air mixing. In order to improve fuel/air mixing, it is important to understand fuel spray formation and its characteristics [1]. Spray characteristics are affected to a great extent by injection process, combustion chamber and nozzle geometry, spray chamber conditions and physical and chemical fuel properties. Nowadays the fuel spray is investigated both microscopically and macroscopically. The first approach takes droplet size and velocity distributions characteristics into consideration, while the second one focuses on the estimation of spray tip penetration, spray area and spray cone angle [2,3]. Therefore, many experimental and numerical investigations are focused on microscopic and macroscopic fuel spray characteristics [4–10]. In recent years, many mathematical models of macroscopic fuel spray characteristics were developed and tested by using both, mineral diesel and alternative fuels at various conditions [11–18].

Spray simulations in non-evaporative conditions show that biodiesel gives a slightly higher spray tip penetration, higher Sauter mean diameter and slightly lower spray angle [19]. Battistoni & Grimaldi [19] concluded that beside fuels the nozzle hole shape has a very important influence on spray characteristics.

In [20] spray characteristics of light and base mineral diesel fuels were investigated under high temperature and high pressure conditions in a constant volume spray chamber. On the basis of experimental results, the authors concluded that fuel sprays of light diesel fuel with low boiling point and low density are short and narrow due to promoted atomization and evaporation with respect to base mineral diesel.

In [21] spray tip penetration, spray angle, spray velocity and spray morphology of biodiesel derived from waste cooking oil were investigated under high injection pressure and high pressure conditions in a constant volume spray chamber. On the basis of experiments, biodiesel shows narrower spray angles than mineral diesel. Furthermore, spray angles were unaffected by injection pressure, but increasing spray chamber pressure resulted in significant increase in spray angles of all fuels. A numerical simulation was conducted by using a new hybrid spray model and Mohan et al. [21] concluded that the obtained results are in good agreement with the experiments.

Agarwal et al. [11] investigated the effect of injection pressure and injection timing on macroscopic spray characteristics in a single cylinder CI engine equipped with high-pressure common rail direct injection system and fueled with karanja biodiesel and mineral diesel. The results showed that higher fuel injection pressure results in a longer spray tip penetration and larger spray area than that at lower injection pressures at same elapsed time after the start of injection. Furthermore, Agarwal et al. [11] showed that average particulate size increased when retarding the injection timing.

Bohl et al. [12] presented the macroscopic spray characteristics of mineral diesel and various biodiesels using constant volume spray vessel at spray chamber pressure of 7 MPa. The results revealed that the lowest fuel density results in shorter spray penetration depth and highest cone angle, enhancing the fuel-air mixture. They concluded that fuel viscosity has an important role in the air fuel mixing process.

* Corresponding author.
E-mail address: breda.kegl@um.si (B. Kegl).

https://doi.org/10.1016/j.fuel.2018.02.169
Received 19 January 2018; Received in revised form 21 February 2018; Accepted 27 February 2018

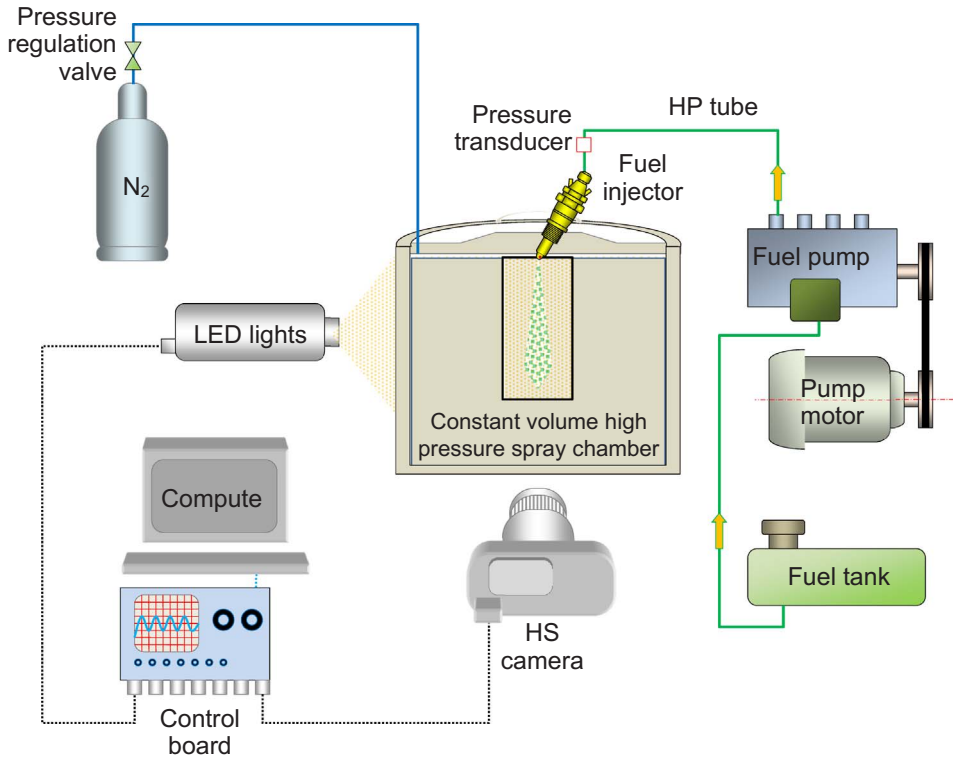

Fig. 1. Spray visualization set-up.

Table 1
Test injection system and high pressure vessel main specifications.

Fuel injection system	
Injection model	Direct injection M system
Fuel injection pump	Bosch PES 6A 95D 410 LS 2542
Pump plunger (diameter × lift)	9.5 mm × 8 mm
Fuel tube (length × diameter)	1024 mm × 1.8 mm
Injection nozzle (number × nozzle hole diameter)	1 × 0.68 mm
Needle lift (maximum)	0.3 mm
Needle opening pressure	17.5 MPa
Pressure in the spray chamber	4 MPa and 6 MPa
Temperature in the spray chamber	294 K

Table 2
Diesel and biodiesel properties.

Fuel	Mineral diesel	Biodiesel
Density @ 30 °C (kg/m^3)	830–835	860–865
Kinematic viscosity @ 30 °C (mm^2/s)	3.34–3.38	4.46–4.49
Surface tension @ 30 °C (N/m)	0.022–0.023	0.024–0.026
Calorific value (MJ/kg)	42–44	38–39
Cetane number	45–50	49–51

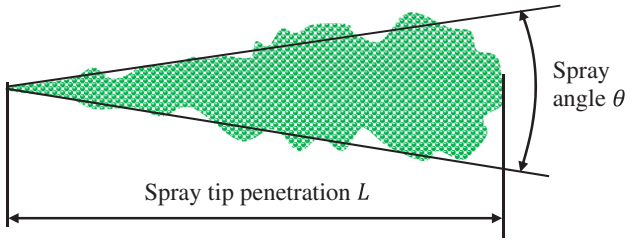

Fig. 2. Spray parameters.

Desantes et al. [13] investigated penetration velocity and radial expansion of reacting fuel spray by using *n*-dodecane, *n*-heptane, and a blend of 80% *n*-heptane and 20% isooctane. A spray model was also applied to support the analysis of experimental results. They concluded that spray tip velocity values under reacting conditions are always larger than under inert ones; for both, experimental and model results.

The period of diesel fuel spray injection from the start of injection up to 0.5 ms was investigated in [22] by using ultrahigh speed digital imaging. In contrast with the widely accepted idea of tip penetration exhibiting a linear dependence with time during the initial stages of spray development, the spray tip penetration was observed as a $t^{\frac{3}{2}}$ dependence until the tip velocity reaches its maximum value. After this, the spray tip penetration correlates well with previously established dependence found in the literature. Kostas et al. [22] concluded that further experiments are required for complete characterization of the fuel spray behavior during the initial phases as well as for interpretation of the functional fit in terms of a physical model.

Roisman et al. [23] modelled the motion of the spray in two regions: the main region of the steady flow and the front region of the spray. Their approach revealed the importance of the shock wave propagation at the initial stage of spray development. Experiments were done on a common rail diesel injection nozzle and numerically predicted results agreed well with experimental data.

Park et al. [24] studied fuel spray characteristics when using diesel water emulsified fuel in a diesel engine. The mean spray penetration length at room temperature was shortened by increased water content. Therefore, diesel water emulsified fuel has a higher probability of wall wetting than neat mineral diesel under the spray chamber pressure of 4 MPa and room temperature. However, the in-cylinder temperature in a running diesel engine is much higher than room temperature. Therefore, one can assume that actual wall wetting would not be significant [24].

Park et al. [15] investigated diesel fuel spray using a constant volume spray chamber under high temperature and high pressure. On the basis of experimentally obtained results, it was shown that the spray

Table 3
Mathematical models for spray tip penetration.

Model	Reference
$L = 1.189 C_c^{0.25}\left(\frac{p_{inj}-p_g}{\rho_g}\right)^{0.25}\left(\frac{d_0 t}{\tan\theta}\right)^{0.5}$	[26]
$L = 3.07\left(\frac{p_{inj}-p_g}{\rho_g}\right)^{0.25}(d_0 t)^{0.5}\left(\frac{294}{T_g}\right)^{0.25}$	[27]
$L = 0.39\left(\frac{2(p_{inj}-p_g)}{\rho_f}\right)^{0.5} t \ldots 0 < t < t_b$	[30]
$L = 2.95\left(\frac{p_{inj}-p_g}{\rho_f}\right)^{0.25}\left(\frac{d_0 t}{1000}\right)^{0.5} \ldots t > t_b$	
$t_b = 28.65\frac{\rho_f d_0}{(\rho_g(p_{inj}-p_g))^{0.5}}$	
$L = 1.141 C_d^{0.5}\left(\frac{p_{inj}-p_g}{\rho_g}\right)^{0.25}\left(\frac{d_0 t}{\tan\theta}\right)^{0.5}$	[28]
$L = 10^{-3} d_0^{0.307} p_{inj}^{0.262} \rho_g^{-0.406} t^{0.568}$	[29]
$L = A t^{\frac{3}{2}} \ldots 0 < t < t_b$	[22]
$L = 2.95\left(\frac{p_{inj}-p_g}{\rho_f}\right)^{0.25}\left(\frac{d_0 t}{1000}\right)^{0.5} \ldots t > t_b$	
$t_b = 29\frac{\rho_f d_0}{(\rho_g(p_{inj}-p_g))^{0.5}}$	
$L = 0.39\left(\frac{2(p_{inj}-p_g)}{\rho_f}\right)^{0.5}\frac{t}{1000} \ldots 0 < t < t_b$	[12]
$L = 0.342\left(\frac{p_{inj}-p_g}{\rho_g}\right)^{0.25}(d_0)^{0.5}\rho_f^{0.3387} t^{0.5432} \ldots t > t_b$	
$t_b = 28.65\frac{\rho_f d_0}{(\rho_g(p_{inj}-p_g))^{0.5}}$	

C_c coefficient of contraction, p_{inj} injection pressure (Pa), p_g spray chamber pressure (Pa), ρ_g gas density in spray chamber (kg/m^3), d_0 nozzle hole diameter (m), t time (ms), θ spray angle (°), T_g gas temperature in chamber (K), ρ_f fuel density (kg/m^3), C_d velocity coefficient, A fit parameter, L spray tip penetration (m).

Table 4
Mathematical models for spray angle.

Model	Reference
$\theta = 2\ \text{atan}\left(\frac{\sqrt{3}}{6}\frac{4\pi\left(\frac{\rho_g}{\rho_f}\right)^{0.5}}{\left(3+0.28\left(\frac{l_0}{d_0}\right)\right)}(1-e^{-10\gamma})\right)$	[31]
$\theta = 0.05\left(\frac{\rho_g(p_{inj}-p_g)d_0^2}{\eta_g^2}\right)^{0.25}$	[32]
$\theta = 2\ \text{atan}\left(\frac{\sqrt{3}}{6}\frac{4\pi\left(\frac{\rho_g}{\rho_f}\right)^{0.5}}{\left(3+0.28\left(\frac{l_0}{d_0}\right)\right)}\right)$	[33]
$\theta = 83.5\left(\frac{l_0}{d_0}\right)^{-0.22}\left(\frac{d_0}{d_{sac}}\right)^{0.15}\left(\frac{\rho_g}{\rho_f}\right)^{0.26}$	[30]
$\theta = 2\ \text{atan}\left(\frac{\sqrt{3}}{6}\frac{4\pi\left(\frac{\rho_g}{\rho_f}\right)^{0.5}}{\left(3+0.28(\frac{l_0}{d_0})\right)}\left(\frac{Re}{We}\right)^{-0.25}(1-e^{-10\gamma})\right)$	[34]
$\theta = 2\ \text{atan}((d_0)^{0.508}(p_{inj})^{0.00943}(\rho_g)^{0.335})$	[29]
$\theta = 2\ \text{atan}\left(C_\theta\left(\left(\frac{\rho_g}{\rho_f}\right)^{0.19} - 0.0043\left(\frac{\rho_f}{\rho_g}\right)^{0.5}\right)\right)$	[35]

$\gamma = \left(\frac{Re}{We}\right)^2\frac{\rho_f}{\rho_g}$; $Re = \frac{v_{inj}d_0}{\nu_f}$; $We = \frac{\rho_f v_{inj}^2 d_0}{\sigma_f}$; $v_{inj} = C_d\sqrt{\frac{2(p_{inj}-p_g)}{\rho_f}}$

ρ_g gas density in spray chamber (kg/m^3), ρ_f fuel density (kg/m^3), l_0 nozzle hole length (m),d_0 nozzle hole diameter (m), d_{sac} diameter of sack chamber (m), v_{inj} injection velocity (m/s), ν_f fuel kinematic viscosity (m^2/s), ν_g gas kinematic viscosity in spray chamber (m^2/s), η_g gas dynamic viscosity (Pas), C_d velocity coefficient, C_θ coefficient depending on the injector characteristics, p_{inj} injection pressure (Pa), p_g spray chamber pressure (Pa), θ spray angle (°).

angle decreases during injection from very high values at the beginning of injection to a practically constant value. Furthermore fuel spray penetration increases due to attenuation of fuel evaporation process and interaction with gas in the spray chamber. A similar development of the spray angle with respect to time was observed by Wang et al. [25].

Although many mathematical models for simulation of macroscopic fuel spray characteristics exist, further investigations of fuel sprays are still necessary due to new alternative fuels and optimized injection systems. For example, till today many models depend greatly on tested fuels and the spray angle after start of injection is not modeled very well. In this paper, attention is focused on the development of a modified model for numerical simulation of spray tip penetration and spray angle by introducing more injection parameters and fuel properties into the model. In order to validate the proposed model, an experimental campaign has been carried out employing both mineral diesel and biodiesel at various chamber pressures. Afterwards, the results have been compared with the existing mathematical models. The analysis of obtained results may contribute to better understanding of the influences of fuel properties on the fuel spray development and consequently on combustion process.

2. Experimental equipment and test procedure

Measurements of macroscopic and microscopic spray characteristics and break-up process was performed in a specially designed high pressure spray chamber, mounted on an injection system test bed, Fig. 1.

The high pressure atmosphere in the injection chamber was created using nitrogen (N_2) from a high pressure vessel. The desired atmosphere pressures of 4 and 6 MPa were adjusted by using a pressure reduction valve. The nitrogen was replaced after each measurement in order to lower the amount of fuel vapor and to avoid fuel splashing on chamber windows. The fuel was delivered by BOSCH PES 6A 95D 410 LS 2542 high pressure pump and injected by BOSCH DLLA 5S834 injector provided with single hole. A data acquisition system (DAQ system) was used for measuring the pressure upstream the injector, the injector needle position and the camshaft angle. A special application needed for the data acquisition was designed in LabVIEW in order to monitor and process all obtained data.

The images of spray morphology development were taken via a digital high speed camera which recorded 18,500 fps at resolution of 128 × 332 pixels. The signal of high speed camera was synchronized with injection test bed DAQ system. This enables to link precisely each photo taken to the pump camshaft angle, needle position, pressures value, etc. High power specially designed LED lights were used for spray illumination in the high pressure spray chamber.

All measurements were performed under full load conditions, determined by the pump rack position. It means that under a single operating regime various fuel properties can cause that fueling is slightly different. Detailed information of the fuel injection system and constant volume high pressure spray chamber is presented in Table 1, meanwhile Table 2 shows the tested fuels properties (mineral diesel and biodiesel from rapeseed oil). The tested biodiesel fuel, produced by Biogoriva Slovenia from rapeseed oil, is compliant with the European standard EN 14214.

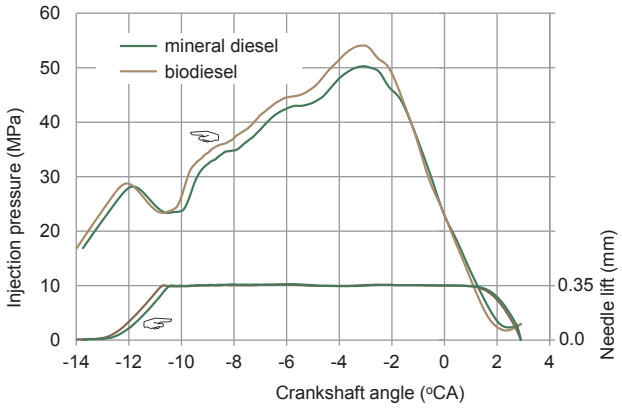

Fig. 3. Injection pressure and needle lift during the injection process.

3. Mathematical models for fuel spray simulation

The most important macroscopic fuel spray characteristics, spray tip penetration L and spray angle θ, are illustrated in Fig. 2. Spray tip penetration is defined as the distance between the nozzle exit and the furthest point of the spray. Spray angle is usually defined as the average angle formed by two straight lines from the nozzle tip to the boundary of the spray.

3.1. Existing mathematical models

Mathematical models for fuel spray characteristics are phenomenological models, obtained by integration of reduced physics based methods and experimental data. For this reason, a lot of mathematical models exist which exhibit rather minor variations; mainly due to various data used for their calibration. The most frequently used models for spray tip penetration and spray angle are assembled in Table 3 and Table 4.

Some models for spray tip penetration are based on one-zone theory [26–29], other models are based on two-zone theory [12,22,30]. At first, Wakuri et al. [26] used momentum theory based on the idea that the air induced into a fuel jet stream results in a kind of mixed gas with fuel droplets. Dent [27] incorporated an additional term of temperatures ratio for the evaporation condition into the correlation equation for sprays produced under non-evaporating condition, to accommodate variation in spray length due to elevated temperature effects. Other one-zone models differ from these two models only in the coefficients or exponent factors of injection, nozzle and spray parameters. Two-zone models use two different equations, one from the beginning of the injection to the jet break-up time, where the penetration is proportional to time, and another one for the time exceeding the jet break-up time, where the penetration is approximately proportional to square root of time. These correlations of spray tip penetration, for liquid and vapor phases, also do not variate significantly between the evaporation and non-evaporation sprays. The first applied two-zone model was developed by Hiroyasu & Arai [30]. This was a starting-point for many other spray models, where the spray tip penetration is calculated from injection, nozzle, spray parameters, and spray chamber conditions.

All existing mathematical models for spray angle deliver more or less constant angles through the whole time of spray development [29,31–35]. Reitz & Bracco [31] as well as Ruiz & Chigier [34] developed a mathematical model for the spray angle by employing the aerodynamic break-up model, which includes the ratio of Reynolds and Weber numbers of the liquid flow. Other models include some characteristics of nozzle and injection parameters, fuels properties, and spray chamber conditions. Existing models differ from each other by different coefficients or exponent factors of included model variables.

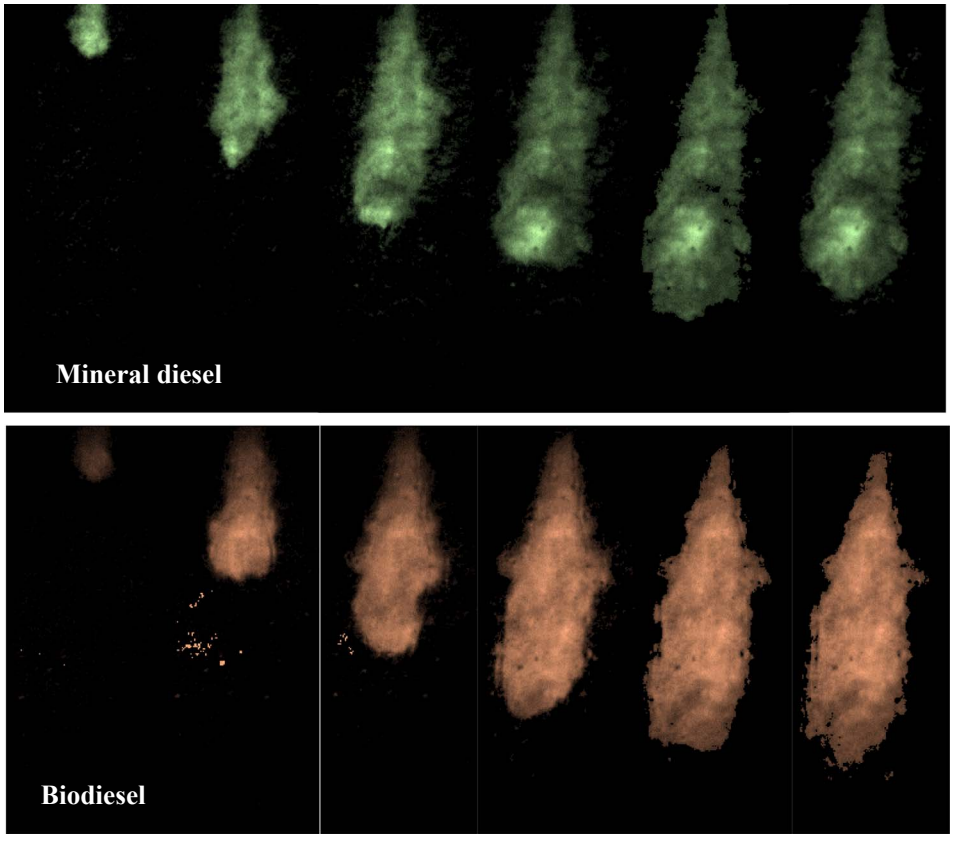

Fig. 4. Images of spray morphology development of mineral diesel and biodiesel; 4 MPa spray chamber.

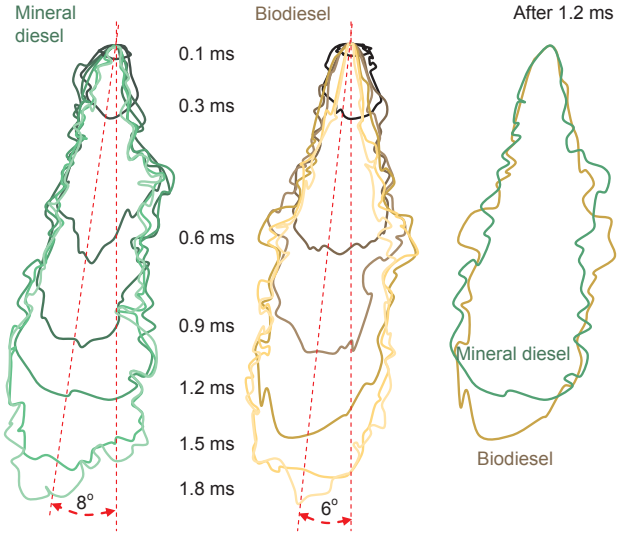

Fig. 5. Spray development of mineral diesel and biodiesel; 4 MPa spray chamber.

3.2. Modified mathematical model

The new model presented in this paper was developed by starting from a set of draft formulas defined by combining terms from existing models. These draft formulas were then enriched by additional terms, formulated intuitively as a result of huge experimental data and experience assembled while performing tests and measurements with various fuels. The resulting model for spray tip penetration and spray angle is based on a two-zone theory. The formula for the break-up time t_b has been somewhat modified with respect to those given in Table 3. Furthermore, the model for spray angle computation includes additional variables, such as: spray length, fuel and gas dynamic viscosity, and fuel surface tension. The spray length term L^{-2} is included into equation (3) because as the spray penetrates, the droplets on the boundaries become smaller and diffuse easily, generating a decreasing trend of spray cone angle [36]. This effect is present only for a short time period after start of injection; therefore this term it is included only within the break-up time. During the break-up time, the gas and fuel dynamic viscosity and fuel surface tension also have an important influence on the spray angle. Therefore, time dependent terms $\left(\frac{\eta_g}{\eta_f}\right)^{0.5t}$ and $\left(\frac{5\cdot10^{-6}}{\sigma_f}\right)^{0.5t}$ are added in order to consider various viscosities and surface tensions of various fuels. After the brake-up time period, the spray angle stabilizes and depends merely on dynamic viscosity; therefore, equation (4) contains the term $\left(\frac{\eta_g}{\eta_f}\right)^{0.25}$. The rather small reduction of the spray angle after the break-up period is taken into account by a linear time dependent term.

Spray tip penetration L (mm) and spray angle θ (°):

$$L = 0.39\left(\frac{2|p_{inj}-p_g|}{\rho_f}\right)^{0.455} t \quad \ldots \quad t < t_b \tag{1}$$

$$L = 92\left(\frac{|p_{inj}-p_g|}{\rho_g}\right)^{0.233} (d_0 t)^{0.5} \quad \ldots \quad t > t_b \tag{2}$$

$$\theta = 0.045\left(\frac{\rho_g \cdot d_0^2 \cdot |p_{inj}-p_g|}{\eta_g^2}\right)^{0.25}\left[\left(\frac{\eta_g}{\eta_f}\right)^{0.5t} + \left(\frac{5\cdot10^{-6}}{\sigma_f}\right)^{0.5t} + L^{-2}\right] \quad \ldots \quad t < t_b \tag{3}$$

$$\theta = 0.12\left(\frac{\rho_g \cdot d_0^2 \cdot |p_{inj}-p_g|}{\eta_g^2}\right)^{0.25}\left[\left(\frac{\eta_g}{\eta_f}\right)^{0.25} - 0.05t\right] \quad \ldots \quad t > t_b \tag{4}$$

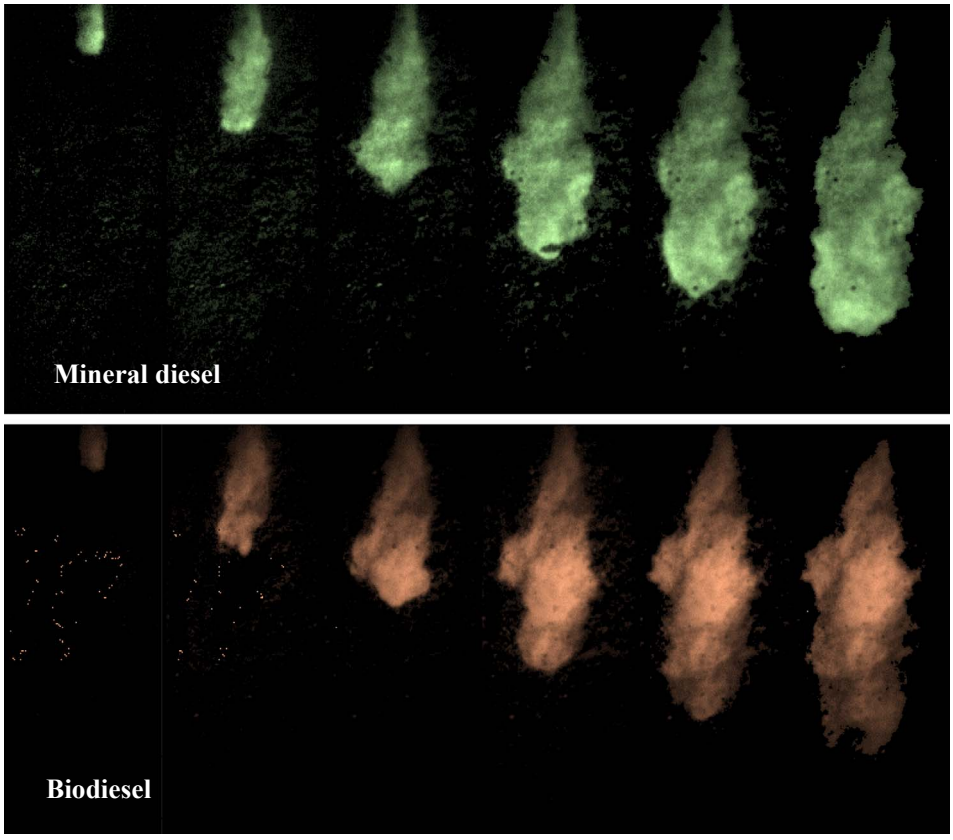

Fig. 6. Images of spray morphology development of mineral diesel and biodiesel; 6 MPa spray chamber.

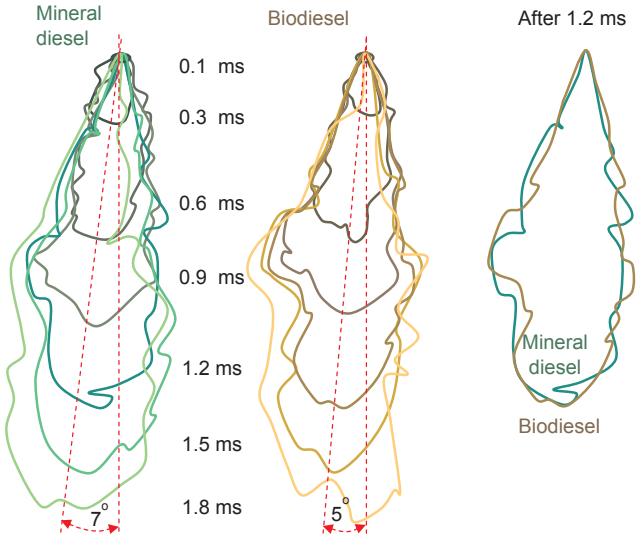

Fig. 7. Spray development of mineral diesel and biodiesel; 6 MPa spray chamber.

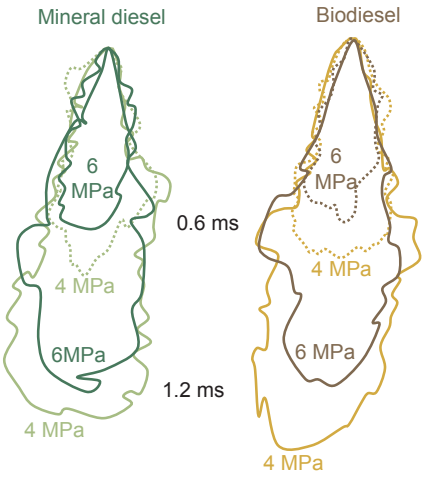

Fig. 8. Spray development at various spray chamber pressures.

where $t_b = 20\frac{\rho_f d_0}{(\rho_g \mid p_{inj} - p_g \mid)^{0.5}}$ is break-up time (ms); t, time after start of injection (ms); p_{inj}, injection pressure (Pa); p_g, spray chamber pressure (Pa); ρ_f, fuel density (kg/m^3), ρ_g, gas density in spray chamber (kg/m^3); d_0, nozzle hole diameter (m), η_f, fuel dynamic viscosity (Pas); η_g, gas dynamic viscosity [Pas], and σ_f, fuel surface tension (N/m).

4. Results and discussion

The experimentally obtained injection pressure and needle lift during injection process are presented in Fig. 3. With respect to mineral diesel, the maximal injection pressure of biodiesel is higher by about 4 MPa and the start of injection is advanced. The higher injection pressure and advanced injection timing by are consequences of higher density and kinematic viscosity of biodiesel, Table 2, as well as of higher sound velocity. The sound velocity of biodiesel is in average about 50 m/s higher than the one of mineral diesel.

The experimentally obtained development of fuel spray in the spray chamber of 4 MPa for mineral diesel and biodiesel at 0.1 ms, 0.3 ms, 0.6 ms, 0.9 ms, 1.2 ms, 1.5 ms, and 1.8 ms after start of injection is presented in Fig. 4 and Fig. 5.

The experimentally obtained development of fuel spray in the spray chamber of 4 MPa for mineral diesel and biodiesel at 0.1 ms, 0.3 ms, 0.6 ms, 0.9 ms, 1.2 ms, 1.5 ms, and 1.8 ms after start of injection is presented in Fig. 4. The spray tip penetration at all times is a little longer for biodiesel due to a somewhat higher injection pressure of biodiesel. It can also be seen that at the beginning of fuel spray development, the spray angle quickly reaches its maximal value but then also quickly decreases and stabilizes at some relatively constant value. Furthermore, it can be seen that the spray angle may be somewhat narrower for biodiesel, compared to mineral diesel; this relation, however, is not observed consistently during spray development. These observations can be explained by various factors. First of all, higher injection pressure increases the spray angle [37]. On the other hand, higher fuel viscosity increases spray evaporation and its velocity and decreases the spray angle [38]. Furthermore, the effects of increased friction between higher viscosity fuel and the nozzle surface reduce by increasing injection pressure. Taking these influences into account, it could can be inferred that spray angles of biodiesel (exhibiting higher injection pressure and higher viscosity) might be very close to mineral diesel.

From Fig. 5, it is evident that there is some angle of inclination of the fuel sprays central axis against the vertical axis corresponding to the

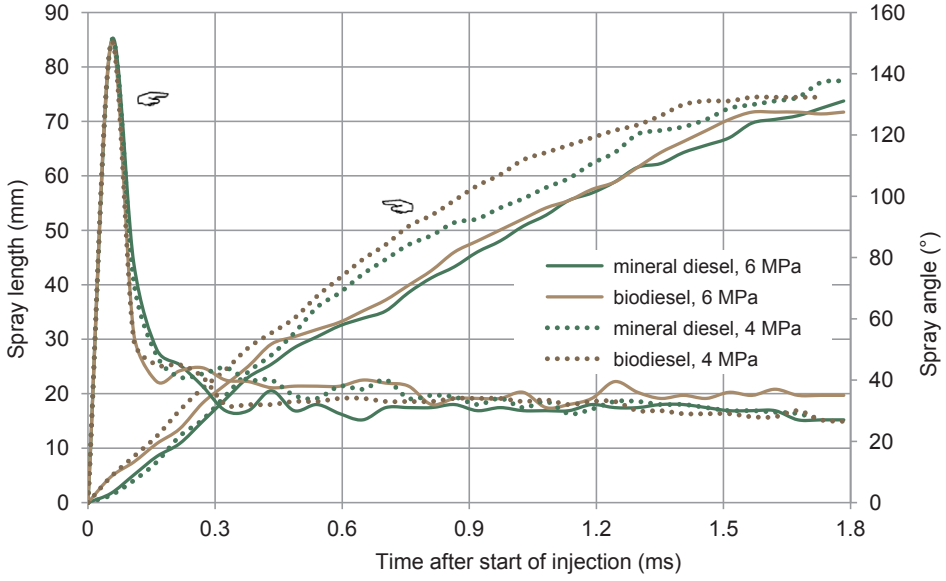

Fig. 9. Spray tip penetration and spray angle; experiment.

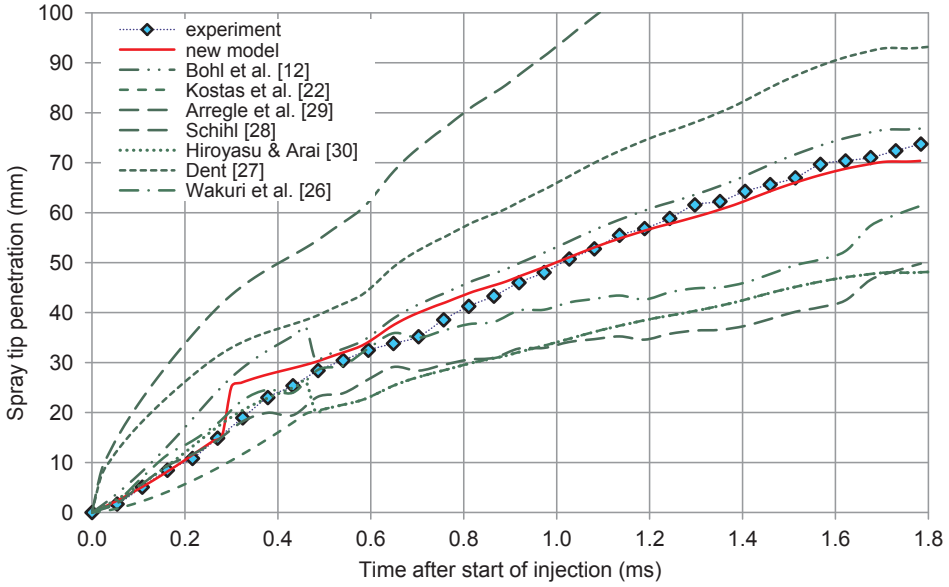

Fig. 10. Spray tip penetration for mineral diesel; 6 MPa spray chamber.

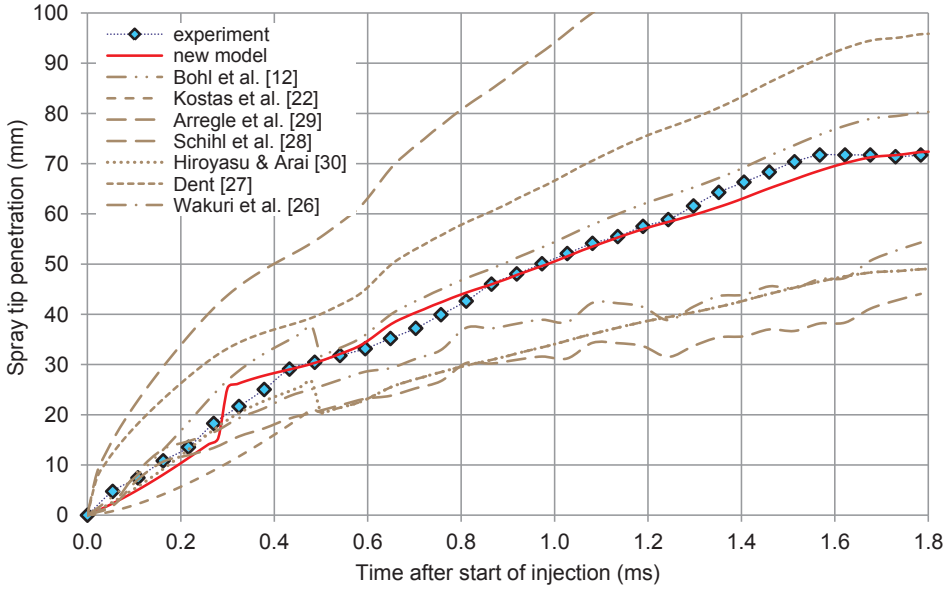

Fig. 11. Spray tip penetration for biodiesel; 6 MPa spray chamber.

geometrical axis of the nozzle hole. It was observed that various fuels resulted in various inclination angles. For mineral diesel these angles were about 8 degrees, while for biodiesel the inclinations were about 6 degrees. The obtained inclination of fuel sprays can be explained by the cavitation inside the injection nozzle hole. It is known that the level of cavitation inside the nozzle hole creates an asymmetry (inclination) of the spray and also leads to much greater spray angles [21]. On the basis of experimental results it can be concluded that a more inclined fuel spray is a consequence of higher cavitation levels in the nozzle hole. Because of larger spray inclination and a somewhat greater spray angle of mineral diesel, it seems that cavitation intensity of mineral diesel is higher than that of biodiesel. This is consistent with the results reported by Agarwal et al. [39] and with the fact that higher viscosity of biodiesel tends to inhibit cavitation inception. At this point it is important to note that cavitation level is not the only important factor; the way of propagation of cavitation area through the nozzle hole is also important. Namely, as the cavitation reaches the nozzle exit, the spray angles become independent of injection pressure and fuel viscosity. When this happens, the spray angle of biodiesel can also become somewhat higher than that of mineral diesel.

Similar results in the development of fuel spray were also obtained in the spray chamber, pressured at 6 MPa, Fig. 6.

The mineral diesel sprays inclinations are about 7 degrees, while the biodiesel spray inclinations are about 5 degrees, Fig. 7.

By comparing the sprays shown in Fig. 5 and Fig. 7, it is evident that at chamber pressure of 4 MPa the inclinations of the sprays are larger than those observed at 6 MPa. It is obvious that higher spray chamber pressure inhibits the cavitation in the nozzle hole, which leads to less inclined fuel spray.

Fig. 8 shows a comparison of spray development at 0.6 ms and 1.2 ms after start of injection for mineral diesel and biodiesel. It can be seen that at 6 MPa the spray tip penetration is shorter than at chamber pressures of 4 MPa; this was observed for both tested fuels. Shorter spray tip penetration at higher chamber pressure is a consequence of higher resistance caused by chamber gas.

Experimentally obtained spray tip penetration and spray angle for

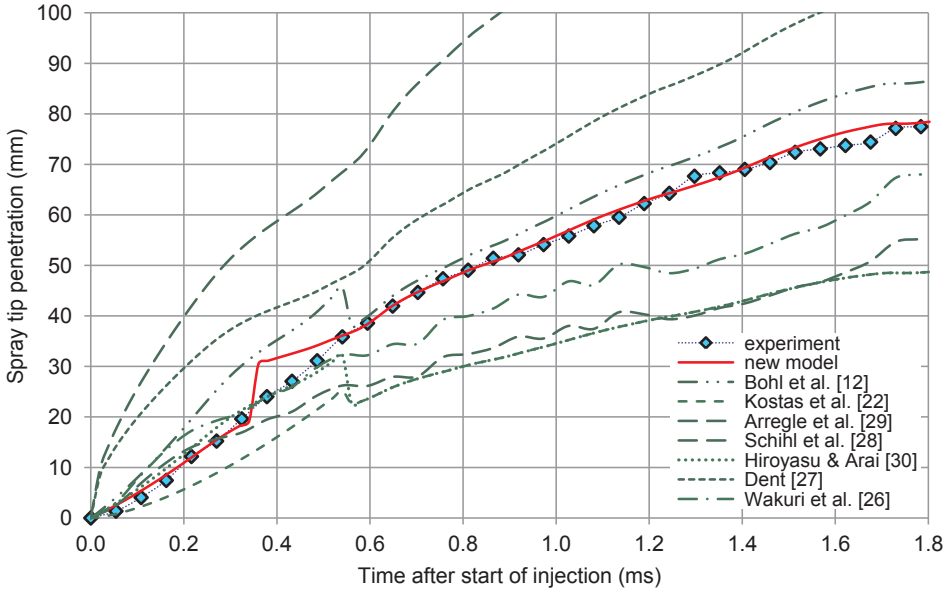

Fig. 12. Spray tip penetration for mineral diesel; 4 MPa spray chamber.

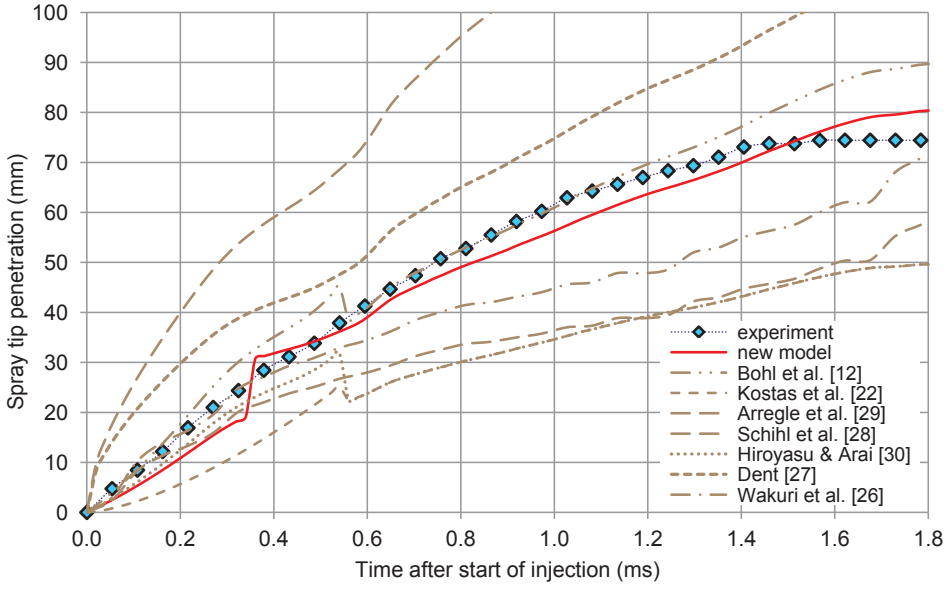

Fig. 13. Spray tip penetration for biodiesel; 4 MPa spray chamber.

mineral diesel and biodiesel (injection into spray chamber at 4 MPa and 6 MPa) are presented in Fig. 9. It can be seen that spray angles increase very rapidly immediately after start of injection; after that they quickly reduce to a practically constant value. This angle reduction is complete about 0.3 ms after the start of injection and the observations are rather similar for both, biodiesel and mineral diesel. A somewhat larger dependence on fuel is observed for spray tip penetration, although chamber pressure is a much more influencing factor.

At this point it might be worth to compare the spray characteristics obtained in high pressure chamber (4 MPa, 6 MPa) with previous results obtained in a low pressure chamber (0.1 MPa) [14]. Regarding spray angle and tip penetration, it can be seen that the differences between mineral diesel and biodiesel are smaller at higher chamber pressures. Namely, at lower pressures the longer and narrower spray of biodiesel is more exposed due to higher viscosity of biodiesel.

The experimental results obtained at 4 and 6 MPa were used to verify the proposed modified numerical model. Spray tip penetration, computed by (Eqs. (1), (2)) as well as by all models given in Table 3, is compared with experiment in Figs. 10–13. Spray angle computed by (Eqs. (3), (4)) and by all mentioned models in Table 4, is compared with experiment in Figs. 14–17.

Fig. 10 shows the comparison for mineral diesel spray at chamber pressure of 6 MPa, meanwhile the comparison for biodiesel is presented in Fig. 11. The comparison of spray length penetration tip at spray chamber pressure of 4 MPa is presented in Fig. 12 for mineral diesel and in Fig. 13 for biodiesel.

Fig. 14 shows the comparison for mineral diesel spray at spray chamber pressure of 6 MPa, meanwhile the comparison for biodiesel is presented in Fig. 15. The comparison of spray angle at spray chamber pressure of 4 MPa is presented in Fig. 16 for mineral diesel and in Fig. 17 for biodiesel.

The results of the modified model for spray tip penetration and spray angle agree very well with the experiments. By introducing the two-zone theory also for the spray angle, it is possible to simulate high angle values at the beginning of injection and rapid angles decrease and stabilization after 0.3 ms.

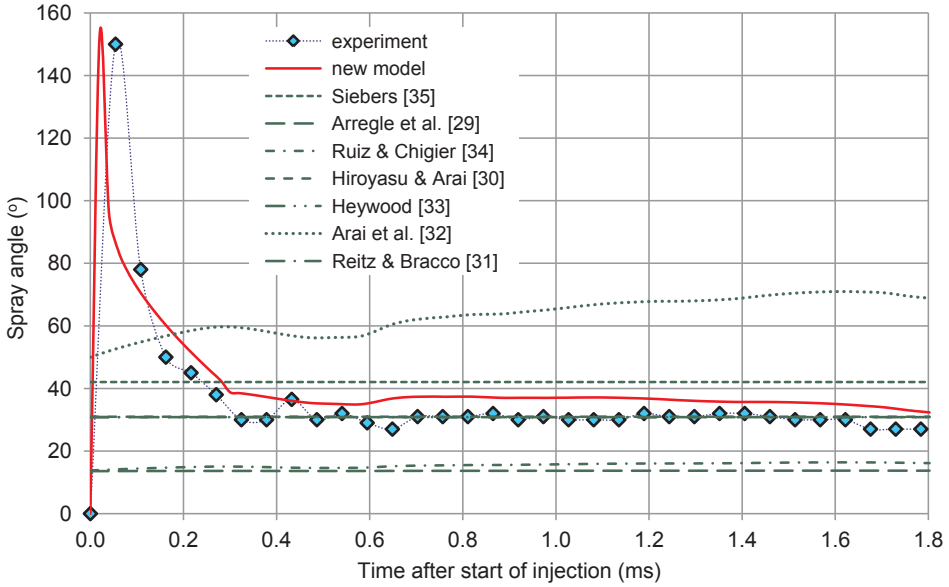

Fig. 14. Spray angle for mineral diesel; 6 MPa spray chamber.

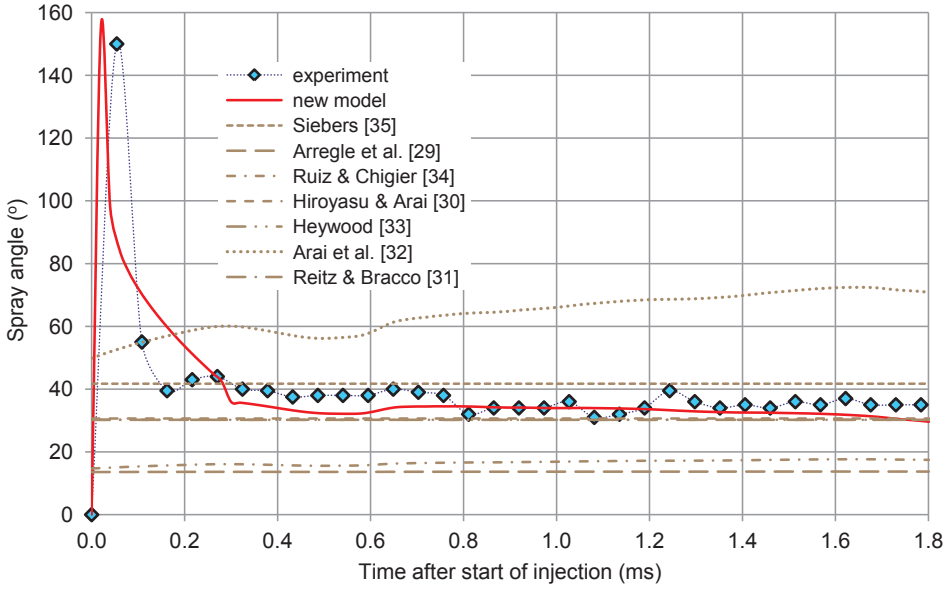

Fig. 15. Spray angle for biodiesel; 6 MPa spray chamber.

It has to be noted that each mathematical model referenced in this work was obtained by fitting it against its corresponding experiments (particular injection system, particular fuels, particular conditions). Therefore differences in the results among various numerical models are a natural consequence of this fact. Nevertheless, one can say that the model proposed in this work delivers very good results under the specified conditions. Furthermore, based on our research it is the only model capable of describing the large angle variation happening immediately after start of injection.

5. Conclusions

The effects of usage of mineral diesel and biodiesel from rapeseed oil on a spray development at spray chamber pressure of 4 MPa and 6 MPa were investigated. A modified mathematical model for spray tip penetration and spray angle is developed and the obtained results were compared with existing mathematical models and with experimental data. From the results, one can conclude the following:

- the inclinations of fuel spray are higher at lower spray chamber pressures, because higher spray chamber pressure inhibits the cavitation in the nozzle hole
- because of higher spray inclination and a somewhat larger spray angle of mineral diesel, it seems that mineral diesel exhibits stronger cavitation than biodiesel
- spray tip penetration at higher spray chamber pressure is shorter than at lower pressures for mineral diesel and biodiesel due to the higher resistance during spray development
- spray tip penetration and spray angle depend more significantly on chamber pressure than on the type of tested fuels
- the developed modified model for spray tip penetration and spray angle delivers results very close to the experimental data; this holds true for mineral diesel and biodiesel as well as for both spray chamber pressures during the whole spray development.

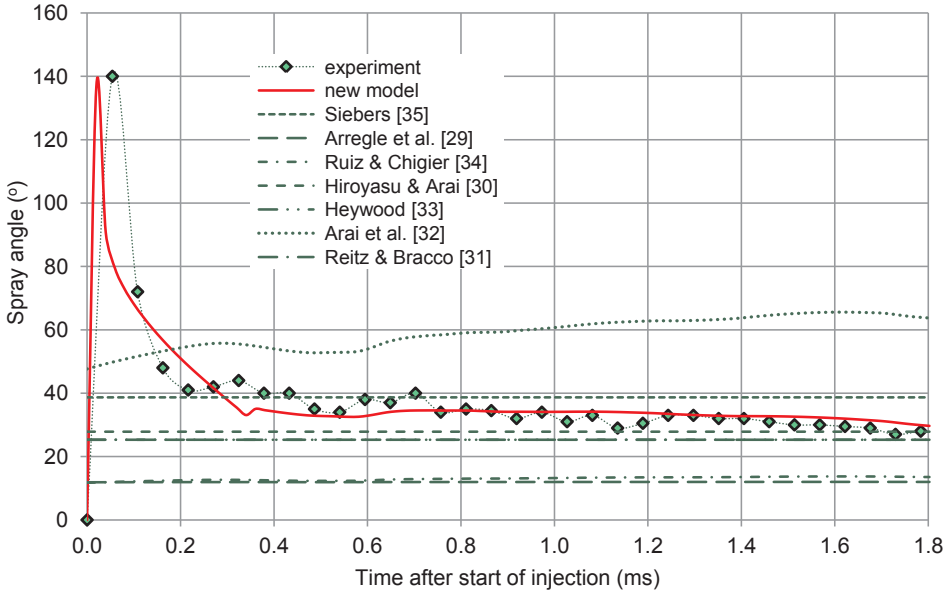

Fig. 16. Spray tip angle for mineral diesel; 4 MPa spray chamber.

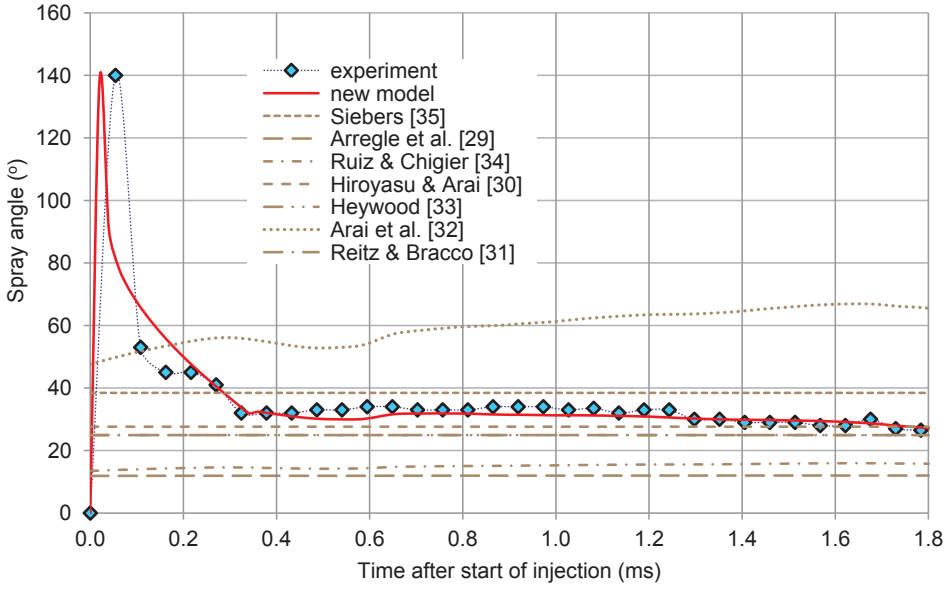

Fig. 17. Spray tip angle for biodiesel; 4 MPa spray chamber.

Acknowledgements

This work was supported by the Slovenian Research Agency (ARRS).

References

[1] Kowalski J. The theoretical investigation on influence the fuel spray geometry on the combustion and emission characteristic of the marine diesel engine. Combust Engines 2017;169(2):101–7.
[2] Kegl B, Kegl M, Pehan S. Green diesel engines: biodiesel usage in diesel engines. London: Springer Verlag; 2013.
[3] Wang Z, Xu H, Jiang C, Wyszynski ML. Experimental study on microscopic and macroscopic characteristics of diesel spray with split injection. Fuel 2016;174:140–52.
[4] Pos R, Wardle R, Cracnell R, Ganippa L. Spatio-temporal evolution of diesel sprays at the early start of injection. Appl Energy 2017;205:391–8.
[5] Park SH, Kim HJ, Lee CS. Numerical investigation of combustion and exhaust emissions characteristics based on experimental spray and atomization characteristics in a compression ignition diesel engine. Energy Fuels 2010;24:2429–38.
[6] Pogorevc P, Kegl B, Škerget L. Diesel and biodiesel fuel spray simulations. Energy Fuels 2008;22:1266–74.
[7] Park SH, Kim HJ, Lee CS. Fuel spray and exhaust emission characteristics of an undiluted soybean oil methyl ester in a diesel engine. Energy Fuels 2010;24:6172–8.
[8] Lanjekar RD, Deshmukh D. Biofuel pure component spray characteristics at engine-relevant conditions. Energy Fuels 2017;31:9438–45.
[9] Ma Y, Hunag S, Huang R, Zhang Y, Xu S. Spray and evaporation characteristics of n-pentanol–diesel blends in a constant volume chamber. Energy Convers Manage 2016;130:240–51.
[10] Wang Z, Guo H, Wang C, Xu H, Li Y. Microscopic level study on the spray impingement process and characteristics. Appl Energy 2017;197:114–23.
[11] Agarwal AK, Dhar A, Gupta JG, Kim WI, Lee CS, Park S. Effect of fuel injection pressure and injection timing on spray characteristics and particulate size–number distribution in a biodiesel fuelled common rail direct injection diesel engine. Appl Energy 2014;130:212–21.
[12] Bohl T, Tian G, Smallbone A, Roskilly AP. Macroscopic spray characteristics of next-generation bio-derived diesel fuels in comparison to mineral diesel. Appl Energy 2017;186:562–73.
[13] Desantes JM, Garciá-Oliver JM, Xuan T, Vera-Tudela W. A study on tip penetration velocity and radial expansion of reacting diesel sprays with different fuels. Fuel 2017;207:323–35.
[14] Kegl B. Influence of biodiesel on engine combustion and emission characteristics. Appl Energy 2011;88:1803–12.
[15] Park Y, Hwang J, Bae C, Kim K, Lee J, Pyo S. Effects of diesel fuel temperature on fuel flow and spray characteristics. Fuel 2015;162:1–7.
[16] Mohan B, Yang W, Yu W, Tay KL. Numerical analysis of spray characteristics of

dimethyl ether and diethyl ether fuel. Appl Energy 2017;185:1403–10.
[17] Wenbin Y, Wenming Y, Mohan B, Lin TK, Feiyang Z. Macroscopic spray characteristics of wide distillation fuel (WDF). Appl Energy 2017;185:1372–82.
[18] Yu Y, Li G, Wang Y, Ding J. Modeling the atomization of high-pressure fuel spray by using a new breakup model. Appl Math Model 2016;40:268–83.
[19] Battistoni M, Grimaldi CN. Numerical analysis of injector flow and spray characteristics from diesel injectors using fossil and biodiesel fuels. Appl Energy 2012;97:656–66.
[20] Lee SW, Tanaka D, Kusaka J, Daisho Y. Effects of diesel fuel characteristics on spray and combustion in a diesel engine. JSAE Rev 2002;23:407–14.
[21] Mohan B, Yang W, Tay KL, Yu W. Experimental study of spray characteristics of biodiesel derived from waste cooking oil. Energy Convers Manage 2014;88:622–32.
[22] Kostas J, Honnery D, Soria J. Time resolved measurements of the initial stages of fuel spray penetration. Fuel 2009;88:2225–37.
[23] Roisman IV, Araneo L, Tropea C. Effect of ambient pressure on penetration of a diesel spray. Int J Multiph Flow 2007;33:904–20.
[24] Park S, Woo S, Kim H, Lee K. The characteristic of spray using diesel water emulsified fuel in a diesel engine. Appl Energy 2016;176:209–20.
[25] Wang Z, Ding H, Ma X, Xu H, Wyszynski ML. Ultra-high speed imaging study of the diesel spray close to the injector tip at the initial opening stage with single injection. Appl Energy 2016;165:335–44.
[26] Wakuri Y, Fujii M, Amitani T, Tsuneya R. Studies of the penetration of a fuel spray in a diesel engine. JSME Int J 1960;3:123–30.
[27] Dent JC. Basis for the comparison of various experimental methods for studying spray penetration, SAE International, SAE paper 710571, 1971.
[28] Schihl P, Bryzik W, Altreya A. Analysis of current spray penetration models and proposal of a phenomenological cone penetration model, SAE International, SAE paper 960773, 1996.
[29] Arrègle JM, Pastor JV, Ruiz S. The Influence of injection parameters on diesel spray characteristics, SAE International, SAE paper 1999-01-0200, 1999.
[30] Hiroyasu H, Arai M. Structures of fuel sprays in diesel engines, SAE International, SAE paper 900475, 1990.
[31] Reitz RD, Bracco FB. On the dependence of spray angle and other spray parameters on nozzle design and operating conditions, SAE International, SAE paper 790494, 1979.
[32] Arai M, Tabata M, Hiroyasu H., Shimizu M. Disintegrating process and spray characterization of fuel jet injected by a diesel nozzle, SAE International, SAE paper 840275, 1984.
[33] Heywood J. Internal combustion engine fundamentals. McGraw-Hill; 1988.
[34] Ruiz F, Chigier N. Parametric experiments on liquid jet atomization spray angle. Atom Sprays 1991;1:23–45.
[35] Siebers DL. Scaling liquid-phase fuel penetration in diesel sprays based on mixing-limited vaporization, SAE International, SAE paper 1999-01-0528, 1999.
[36] Chen PC, Wang WC, Roberts WL, Fang T. Spray and atomization of diesel fuel and its alternatives from a single-hole injector using a common rail fuel injection system. Fuel 2013;103:850–61.
[37] Yan F, Du Y, Wang L, Tang W, Zhang J, Liu B, et al. Effects of injection pressure on cavitation and spray in marine diesel engine. Int J Spray Combust Dyn 2017;9(3):186–98.
[38] Sagar SK, Sabarinath R, Narendran R, Gowtham M, Boobalasenthilraj AK, Raghu P. Experimental investigation on fuel spray parameters and characteristics of diesel and bio-diesel blend. Int J Adv Res Basic Eng Sci Technol 2017;3(33):129–35.
[39] Agarwal AK, Som S, Shukla PC, Goyal H, Longman D. In-nozzle flow and spray characteristics for mineral diesel, Karanja and Jatropha biodiesels. Appl Energy 2015;156:138–48.